Shallow Shear Wave Velocity Structure of the Charleston Historical District, South Carolina: Comparison of Surficial Methods and Borehole Results

USGS Grant 05HQGR0072

Steven C. Jaume, Norman Levine, Christopher H. Brown[1] and Sarah Louise Cooper[1]
Department of Geology and Environmental Geosciences
College of Charleston
66 George Street
Charleston, SC 29424
Telephone: (843) 953-1802
FAX: (843) 953-5446
Email: jaumes@cofc.edu
[1]Undergraduate students

Program Element: I
Keywords: Shear wave velocity, seismic refraction, refraction microtremor, borehole geophysics

Investigations Undertaken

The greater Charleston, South Carolina region was severely damaged by the largest earthquake in the southeastern United States, the M = 6.9-7.3 earthquake of August 31, 1886 (Johnston, 1996; Bakun and Hopper, 2004). Persistent low-level seismicity combined with paleoliquefaction evidence suggesting a repeat time of 500-600 years (Talwani and Schaeffer, 2001) is reflected in the Charleston, SC region having the second highest seismic hazard east of the Rocky Mountains (Frankel et al., 2002).

Earthquake ground motion at a particular location is strongly influenced by shallow geologic structure modifying the incoming seismic wave motion. Robinson and Talwani (1983) found that both building construction (brick versus wood frame) and site conditions (made versus solid ground) played a role in determining damage distribution during the 1886 earthquake. Determining the shear wave velocity structure of a site has proven to be an effective input into predicting how these "site effects" influence the actual ground motion. However, recovering well-constrained shear wave velocity information has most often required relatively time consuming and expensive drilling and logging of boreholes. In FY2005 our research focused upon collecting and interpreting surficial seismic data for shear wave velocity structure. In particular we collected ambient seismic noise data and used a new technique termed "Refraction Microtremor" or ReMi (Louie, 2001) to determine shear wave velocity structure at 21 sites where Seismic Cone Penetration Test (SCPT, i.e., borehole) data already exist (Figure 1).

We selected sites for the seismic data collection based a database of SCPT results and locations reported in a previous NEHRP study by Chapman et al. (2003). Martin Chapman also shared additional notes describing the site locations. The latitude and longitude information for the SCPT sites was incorporated into a GIS product that included relatively recent (1999) aerial photographs and a road network database. Based upon this initial review it was apparent that some latitude and longitude information was

incorrect; i.e., sites documented as being next to building sites were located in the midst of marshes, etc. Consultation with Martin Chapman revealed that his team had difficulty in remotely locating some sites from field report maps made when the original SCPT work was done (Note: Due to the rapid growth of the Charleston metropolitan area many new streets and structures do not appear on publicly available geographic databases). Therefore, we visited the local offices of two firms who conducted most of the original SCPT work (S&ME and Wright Padgett & Christopher) and were graciously allowed to photocopy maps from the field reports. With this information in hand we were able to more accurately locate some SCPT boreholes and even determine the location of three SCPT sites that Chapman et al. (2003) were unable to find (Figure 1).

Sites were chosen for seismic data collection primarily on the availability of space to deploy a seismic refraction line of at least 60 meters in length. This minimum length was chosen as the approximate length needed to define the shear wave velocity structure to a depth of 30 meters using the ReMi technique. In practice we deployed geophones along lines ranging from 80.5 to 184 meters (i.e., 24 geophones spaced at 3.5 to 8 meters). At all 21 sites we collected P-wave refraction data using a sledgehammer source and vertical 4.5 Hz geophones. J. Louie (pers,. comm.) has noted that using a P-velocity model as a constraint improves the shear wave velocity model interpreted using the ReMi technique when the Poisson's ratio of the sedimentary material is significantly greater than 0.25 (i.e., a P vs. S velocity ratio >> 2). These were reversed profiles at 20 sites; due to equipment problems we did not collect a reversed profile at one site (see Table 1 for details of data collected at each site). We also collected shear wave refraction data at seven sites (Table 1) using horizontal 4.5 Hz geophones. The shear wave source consisted of a block of wood pinned beneath a vehicle tire and struck horizontally by a sledgehammer. Six of the seven shear wave refraction lines are reversed profiles. At all 21 sites we recorded six or twelve 30-second long ambient seismic noise profiles using both the vertical and horizontal geophones. In all of the above cases we deployed the geophones on the ground surface; i.e., spiked as firmly as possible into the soil. Given our goal of accessing the ReMi technique as a means of rapid site assessment we did not bury the geophones. It was noted that at several sites extremely loose or compact soil did not allow for good geophone coupling. At several sites (Table 1) we also deployed geophones on a hard surface (asphalt or concrete) by detaching the spikes and placing the geophones upon common red bricks. We collected only ambient noise data in this manner. During our SCPT site location investigation phase we noted that at several SCPT sites (primarily in downtown Charleston) there was no available space to deploy geophones on a soil surface. Thus we wanted to have some ambient noise data collected on a hard surface to compare with data collected using geophones coupled to the soil, to determine if the ReMi technique performs well under these conditions.

All seismic data were originally collected in SEG-2 format. We also converted this data to SEG-Y format to allow for more flexibility in analysis and interpretation. We plan to make this data available online in both formats as a Web-GIS product we are in the process of developing.

The P- and shear wave refraction data were initially interpreted using the RAS-24 software used in the field data collection. This software allows one to pick first breaks and estimate velocities along linear first arrival segments. However, this software does not have filtering options that are useful in the high cultural noise environment in which

the data was collected. Therefore we also used the Resource Geology Seismic Processing System for Java (JRG) (J. Louie, pers. comm.), which allows for bandpass filtering and first break picking of the refraction data (Figure 2). First break picks were exported into MS Excel and interpreted using slope and intercept for a layered velocity structure (Figure 3). In a number of cases there are apparent dipping layers in the shallow velocity structure (Figure 4).

The ambient seismic noise data were interpreted using SeisOpt ReMi™. The seismic traces are converted into p-tau (slowness-intercept time) space and a Fast Fourier Transform is applied to the tau domain to create a p-f (slowness-frequency) image of the ambient seismic energy (see Louie, 2001 for details). The p-f image is then interpreted in terms of a Rayleigh dispersion curve, where an increase in spectral energy at large slowness (slowest velocity) is interpreted as Rayleigh waves traveling parallel to the line of sensors (Figure 5). A second module allows one to interpret the resulting Rayleigh dispersion curve in terms of a layered shear wave velocity structure based upon an algorithm by Saito (1979; Figure 6). This module allows one to adjust both Vp and Vs of a layered structure, plus the density. For our interpretations, we left the density at its default value of 2.0 g/cm^3. We constructed ambient noise derived shear wave velocity models for each site in two ways: 1) by simply adjusting shear velocities (assuming a Vp/Vs ratio of 1.73) and layer thicknesses until we matched the Rayleigh dispersion picks, and 2) first fixing the Vp structure based upon the refraction results and then adjusting shear wave velocities only. Figure 7 shows the difference in the resulting velocity models for site S01469.

Results

Our analysis of the data collected during summer 2005 is only partially complete. The results described below are based upon this partial work; the conclusions are tentative and may change as all the data is fully analyzed.

In terms of compressional velocities, our results are very similar to those of Odum et al (2003) for their sites in and near Charleston. The shallow soil Vp ranged from 182 to 404 m/sec. Vp increased to near 1500 m/sec or more at depths ranging from 1.3 to 3.9 meters, which we interpret as the depth to the local water table. The maximum Vp encountered was 2667 m/sec at a depth of 15 meters.

Because of high levels of cultural noise, we were only able to make useful first break picks at six of the seven sites where we collected shear wave refraction data. At these sites the surficial shear wave velocities ranged from 178 to 257 m/sec. A maximum refraction-derived shear wave velocity of 525 m/sec was recovered at a depth of only 5 meters. These results are also comparable to that of Odum et al. (2003).

Up to six sets (each of six 30-second long records) of ambient noise data were collected at each site (Table 1). We examined the individual p-f images from each set, selecting those that gave the clearest image (i.e., sharpest break between purple colors representing no seismic energy and the start of a clear increase in seismic energy at each frequency, Figure 5). We combined these individual selected images into a final image from which we picked the Rayleigh dispersion values. For this initial work we chose whichever set (vertical or horizontal sensors; grass or bricks) gave the clearest p-f images for the interpretation. We will compare the results using the different sensor types and setups in future work.

As noted above, we constructed Vs models both with and without a Vp model constraint. We found that the shear wave velocity structures derived in these two fashions were systematically different. In general, the depth to first major velocity increase was deeper and magnitude of the velocity change was reduced (Figure 7) when the Vp constraint was used. In addition, we generally find lower shear wave velocities in the deeper layers. This is also results in a systematic decrease in the V_{S30} at each site (Figure 8), which is fit well by simply decreasing V_{S30} by ~ 42 m/sec.

The overall purpose of this work was to compare the Vs structure derived from the surficial seismic methods to SCPT borehole information. Unfortunately most of the available SCPT tests are relatively shallow; most less than 30 meters and many less than 20 meters. In Figure 9 we compare the Vs structure at 4 sites where both SCPT (depths ≥ 23 meters) and ReMi results are available. While differing in detail, we find that the SCPT and ReMi velocity structures are similar and the estimated V_{S30} agree within 10%..

Our initial results strongly suggest that the refraction microtremor method yields shear wave velocity structures and V_{S30} comparable to the SCPT method, as long as a Vp model constraint is used. In lieu of a Vp model, we also find that the refraction microtremor provides an accurate V_{S30} estimate if a correction is applied, which we estimate as –42 m/sec in our study region.

We plan to conduct more detailed analyses of the seismic data and examine how our estimated V_{S30} correlates with surface geology, etc., in future work. We will also finish constructing a Web-GIS product that will allow users to examine our results and the SCPT data from each site investigated, in addition to downloading the field seismic data for further analysis.

References

Bakun, W. H., and M. G. Hopper (2004). Magnitudes and locations of the 1811-1812 New Madrid, Missouri and the 1886 Charleston, South Carolina earthquakes, Bull. Seism. Soc. Amer. **94**, 64-75.

Chapman, M. C., J. R. Martin, G. Olgun and B. Regmi (2003). Prediction and geographical information system (GIS) mapping of ground motions and site response in Charleston, SC and two neighboring counties: first phase development of a GIS for seismic hazard evaluation, final report, USGS Grant 00HQGR0036.

Frankel, A. D., Petersen, M. D., Mueller, C. S., Haller, K. M., Wheeler, R. L., Leyendecker, E. V., Wesson, R. L., Harmsen, S. C., Cramer, C. H., Perkins, D. M., and K. S. Rukstales (2002). Documentation for the 2002 update of the national seismic hazard maps, U.S.G.S. Open-File Rpt. 02-240, 33 pp.

Johnston, A. C. (1996). Seismic moment assessment of earthquakes in stable continental regions, III. New Madrid 1811-1812, Charleston 1886, and Lisbon 1755, Geophys. J. Int. **126**, 314-344.

Louie, J. N. (2001). Faster, better shear-wave velocity to 100 meters depth from refraction microtremor arrays, Bull. Seism. Soc. Amer. **91**, 347-364.

Odum, J. K., R. A. Williams, W. J. Stephenson and D. M. Worley (2003). Near surface S-wave and P-wave seismic velocities of primary geological formations on the Piedmont and Atlantic coastal plain of South Carolina, USA, USGS Open File Report **03-343**.

Robinson, A., and P. Talwani (1983). Building damage at Charleston, South Carolina, associated with the 1868 earthquake, Bull. Seism. Soc. Amer. **73**, 633-652.

Saito, M. (1979). Computations of reflectivity and surface wave dispersion curves for a layered media. I. Sound wave and SH wave, Butsuri-Tanko **32**, 15-26.

Talwani, P., and W. T. Schaeffer (2001). Recurrence rates of large earthquakes in the South Carolina coastal plain based on paleoliquefaction data, J. Geophys. Res. **106**, 6621-6642.

Table 1: Locations of field sites and data collected during summer 2005. Site codes allow reference to SCPT data in the database of Chapman et al. (2003). R = reversed profile; NR = non-reversed profile; numbers represent number of 30 second ambient noise samples taken at each site.

Site Code	Latitude	Longitude	P refraction	S refraction	Vertical (soil)	Vertical (brick)	Horizontal (soil)	Horizontal (brick)
dnv3	32.8873	-80.0104	R		6		6	
dnv4	32.8524	-79.8853	R		6	6	6	
s99140	32.9721	-80.0485	R		6		6	
s99526	32.7521	-80.0285	R		6		6	
s01039	32.7936	-79.9558	R	R	6		6	
s01469	32.9438	-80.0566	R	R	6	6	6	
s01772	32.8026	-79.8979	R		6		6	
s02105	32.789	-79.926	R	R	6		6	
s02290	32.81	-80.0451	R		6	6	6	6
w01122	32.7968	-79.8588	R		6		6	
w01187	32.879	-79.8242	R		6		6	
w01239	32.8419	-79.8123	R	NR	6		6	
w01243	32.8369	-80.0893	R	R	6	6	6	6
w01252	32.8974	-79.7792	R	R	12	6	12	6
w01277	32.8066	-79.8893	R		6		6	
w01317	32.7102	-79.9648	R		6		6	
w02044	32.7497	-80.0353	R	R	6		6	
w02059	32.926	-80.0659	R		6		6	
w02073	32.9608	-80.0599	R		6		6	
w02096	32.6161	-80.1408	R		6		6	
w02104	32.9061	-79.9174	NR		6		6	

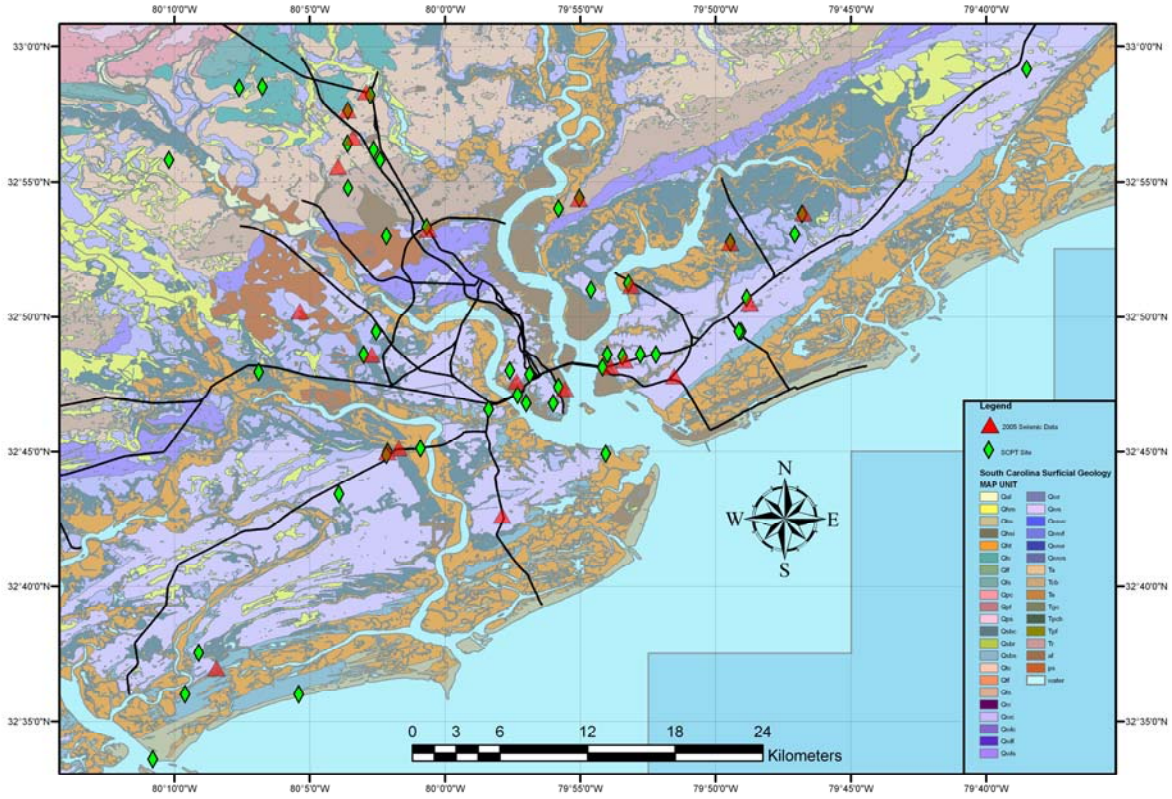

Figure 1: Map of study area showing surface geology, seismic data collections sites (red triangles) and SCPT boreholes (green diamonds) from the database of Chapman et al. (2003). Note that all seismic data collection was conducted near SCPT sites but several either did not have locations in the Chapman et al. (2003) database or were mislocated.

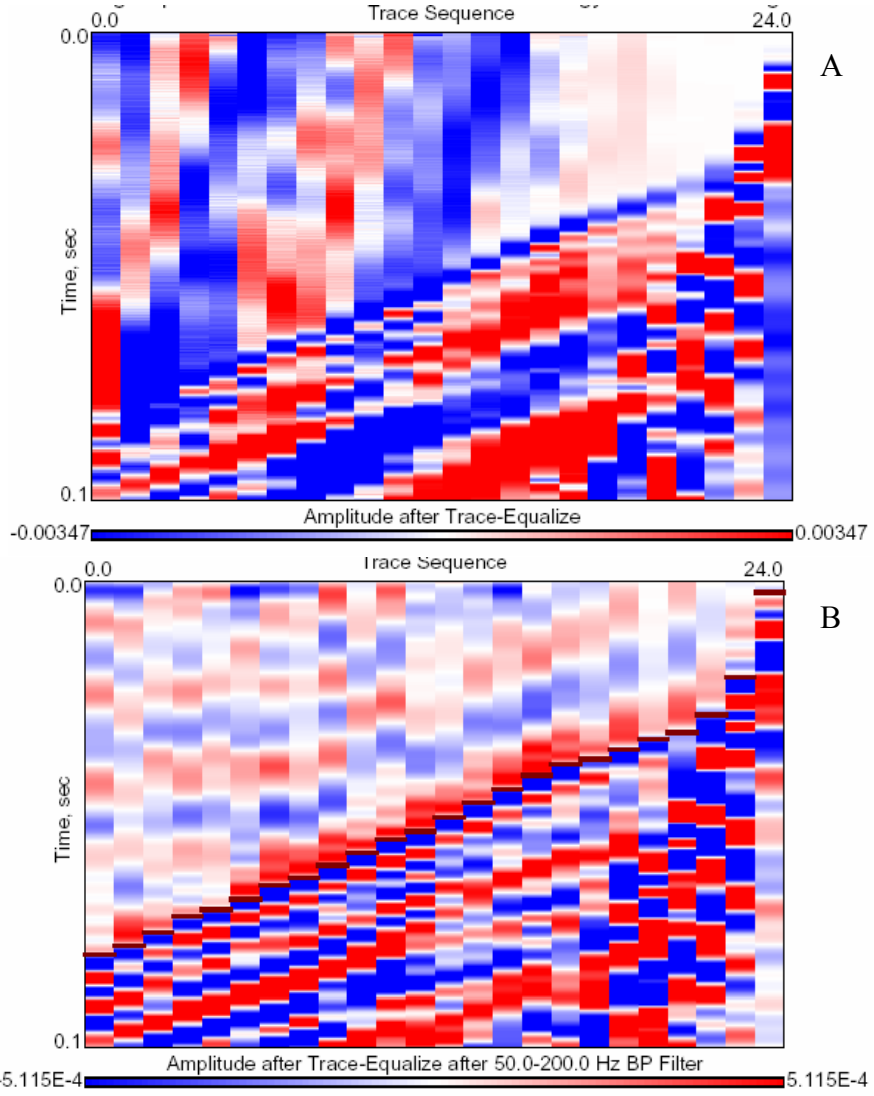

Figure 2 A, B.

A) Top: Example of unfiltered P refraction data displayed in the Resource Geology Seismic Processing System for Java (JRG) system. Source was 6 stacked vertical hammer shots (right side).

B) Bottom: Same data bandpass filtered between 50 and 200 Hz. First break picks are shown as dark red bars.

Figure 3: Example P refraction first arrival time versus distance. In this case the data defines a simple two-layer structure, which we interpret as having Vp = 304 m/sec down to 3.6 meters and 1662 m/sec at greater depths.

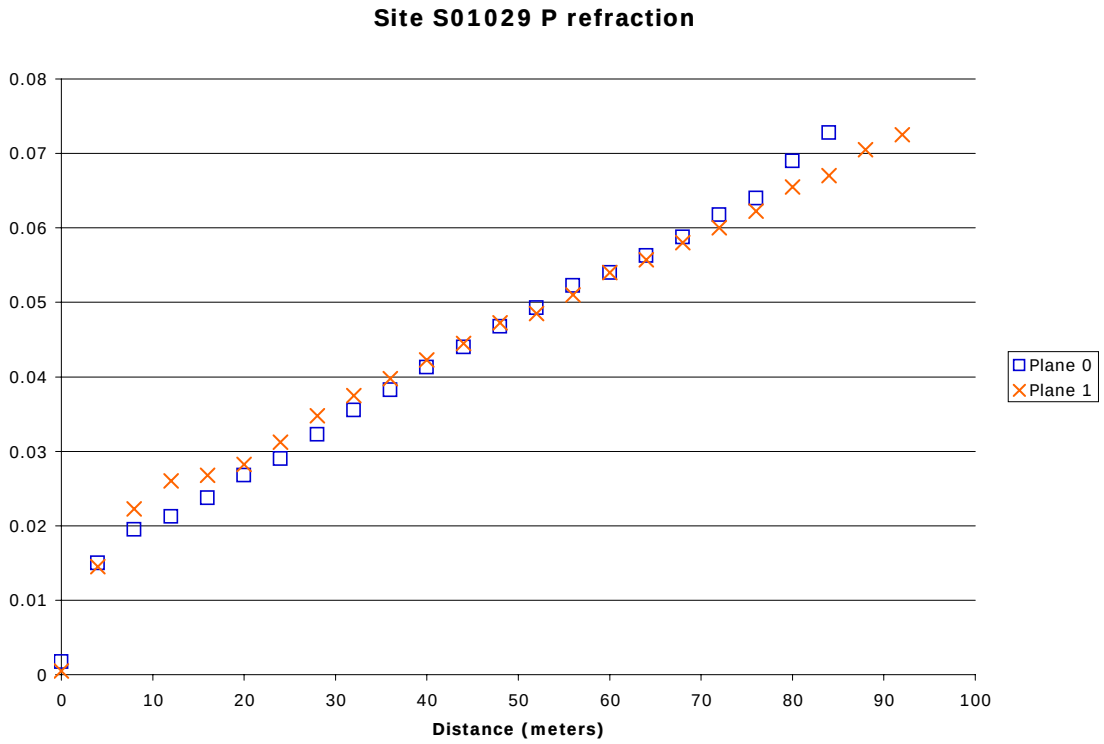

Figure 4: P refraction first arrival times from site S01029. In this case the first arrival times define a slightly dipping (~1°) two-layer structure, with Vp = 294 m/sec in the upper layer and Vp = 1556 m/sec for the deeper layer. The depth to the interface ranges from 2.04 to 2.60 meters.

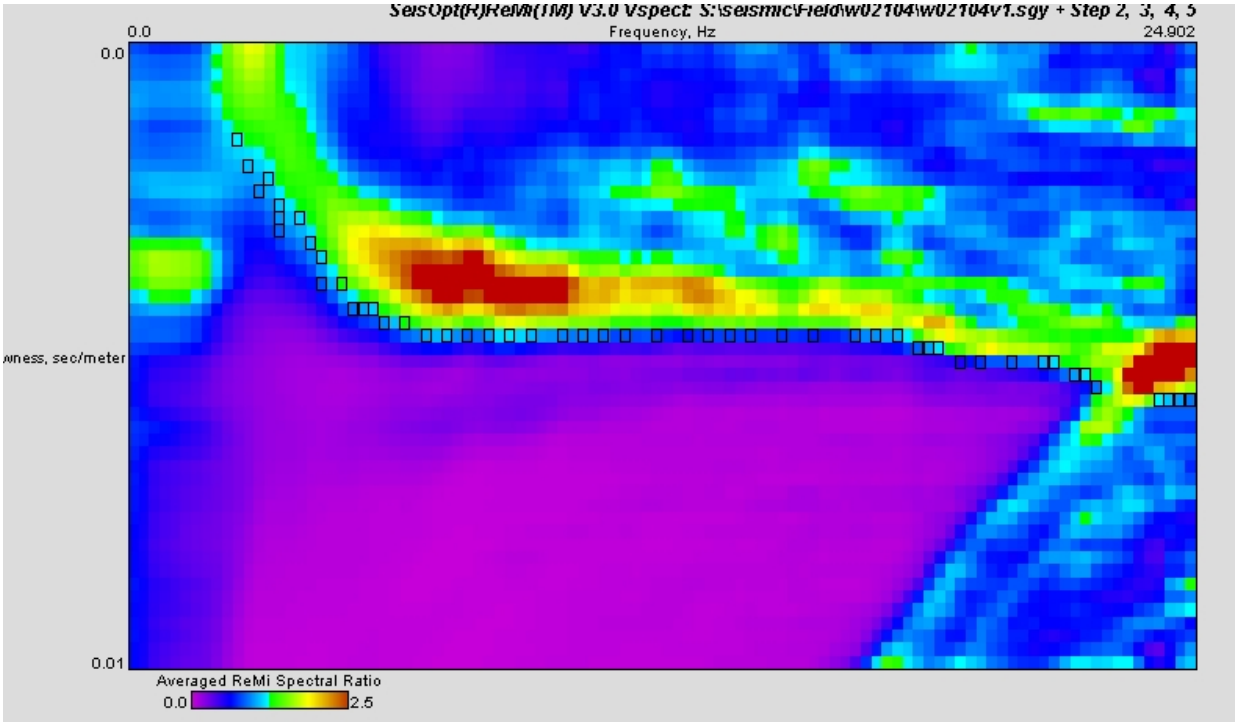

Figure 5: Example p-f diagram of processed ambient seismic noise recorded with vertical geophones at site W02104. The boundary between very low spectral energy (violet) and a sharp increase in spectral energy is interpreted as the Rayleigh dispersion curve for the site. Boxes are picked dispersion values used to model the site velocity structure.

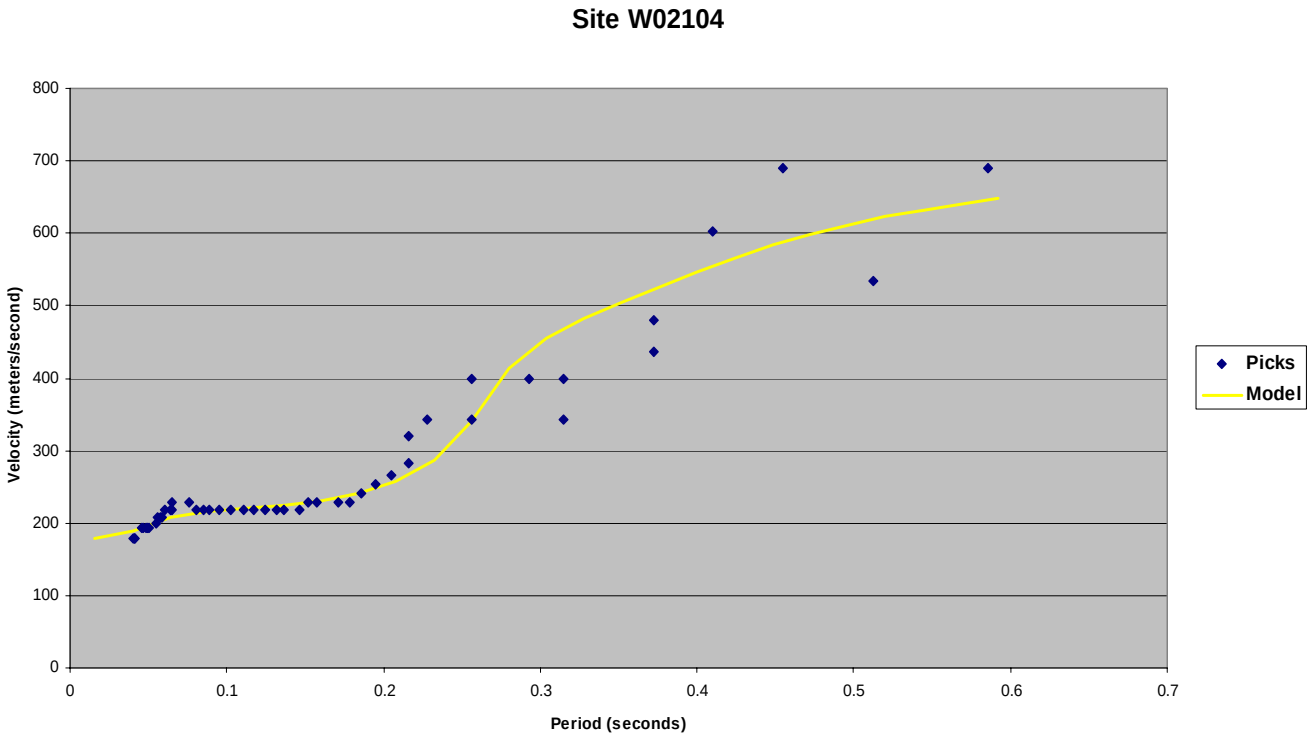

Figure 6: Example of a model fit to the Rayleigh dispersion curve from site W02104.

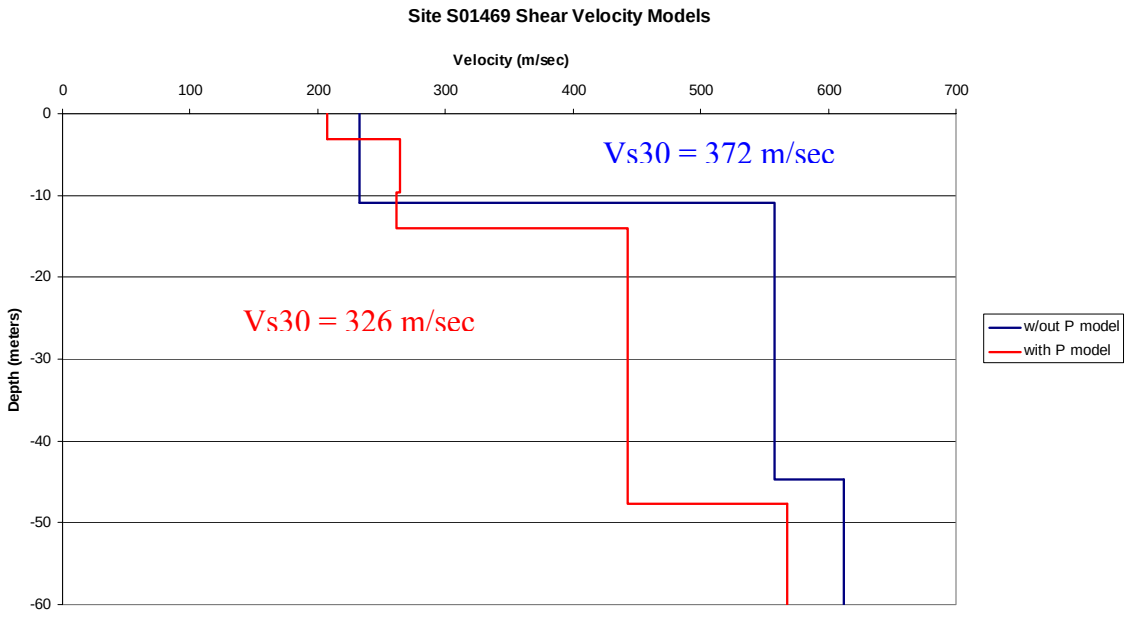

Figure 7: Ambient noise derived shear wave velocity models for site S01469. This site shows the typical result of including a P-velocity model constraint in modeling the ambient noise; i.e., an increase in the estimated depth of the first major velocity increase and a general decrease in velocity of the deeper layers, resulting in a lower V_{S30}.

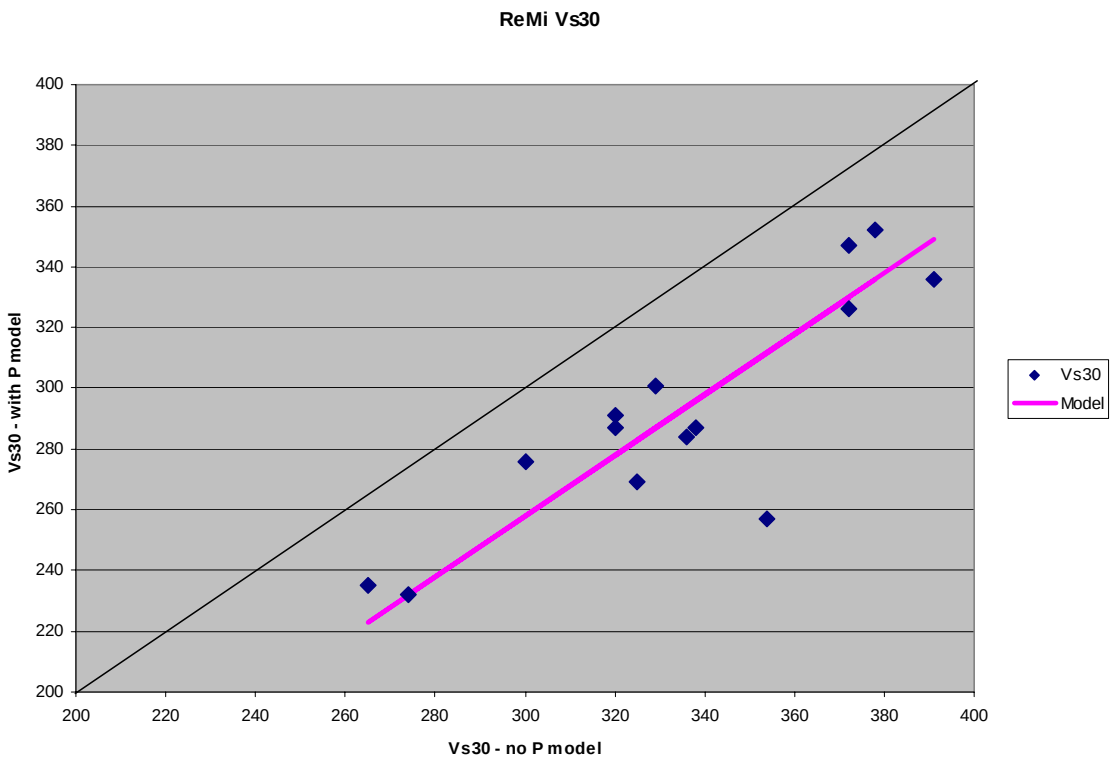

Figure 8: Comparison of V_{S30} estimated from ambient seismic noise when a P-velocity model constraint is used versus when it is not. We find that V_{S30} is systematically lower when the P-velocity constraint is used. This difference appears to be adequately described by a constant decrease of 42 m/sec.

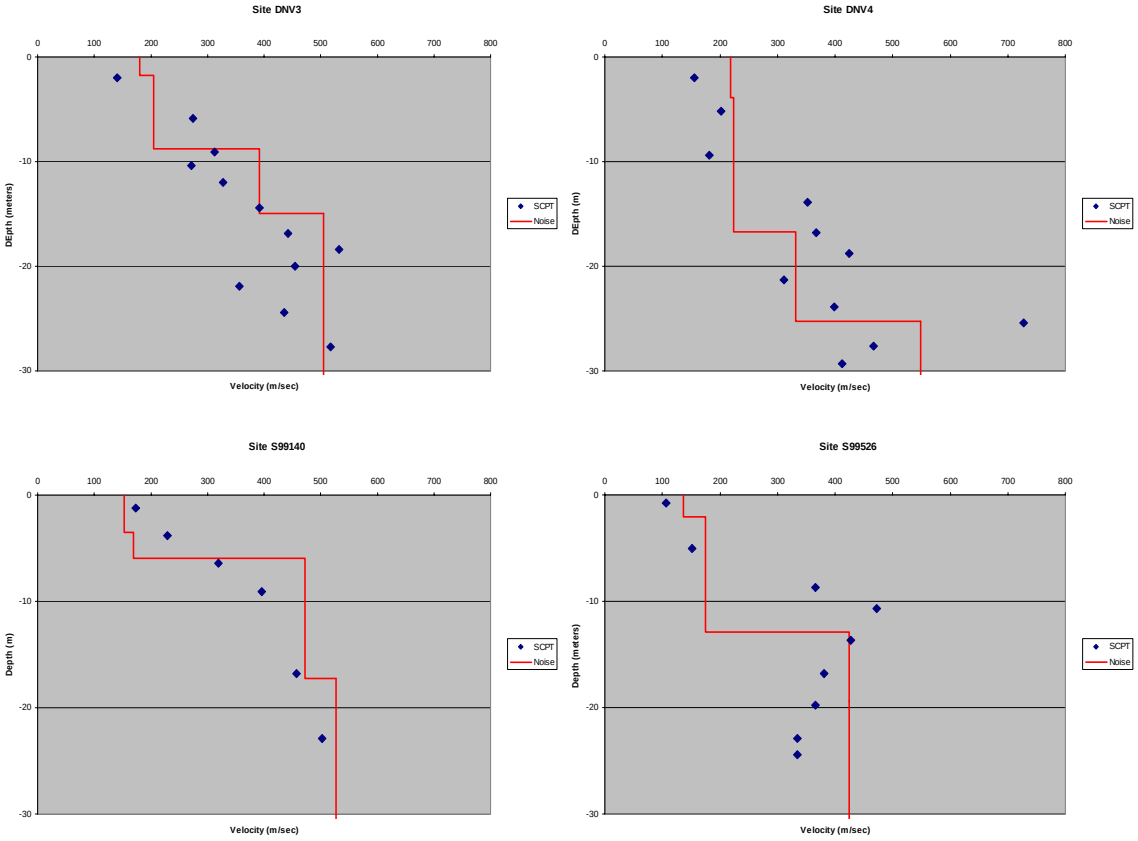

Figure 9: SCPT velocities (blue circles) versus ReMi derived velocities (red lines) at four deep SCPT sites in the Charleston region.